

# UCSF

## UC San Francisco Previously Published Works

### Title

Sex-specific epigenetic profile of inner cell mass of mice conceived in vivo or by IVF

### Permalink

<https://escholarship.org/uc/item/5tc7f1h7>

### Journal

Molecular Human Reproduction, 26(11)

### ISSN

1360-9947

### Authors

Ruggeri, Elena  
Lira-Albarrán, Saúl  
Grow, Edward J  
et al.

### Publication Date

2020-11-01

### DOI


10.1093/molehr/gaaa064

Peer reviewed

# Sex-specific epigenetic profile of inner cell mass of mice conceived *in vivo* or by IVF

Elena Ruggeri<sup>1,2</sup>, Saúl Lira-Albarrán<sup>1</sup>, Edward J. Grow<sup>3</sup>, Xiaowei Liu<sup>1</sup>, Royce Harner<sup>1</sup>, Emin Maltepe<sup>4</sup>, Miguel Ramalho-Santos<sup>1,5,6</sup>, Annemarie Donjacour<sup>1</sup>, and Paolo Rinaudo<sup>1,\*</sup>

<sup>1</sup>Department of Obstetrics, Gynecology and Reproductive Sciences, University of California, San Francisco, CA, 94143, USA <sup>2</sup>San Diego Zoo Global, Institute for Conservation Research, Reproductive Sciences, Escondido, CA, 92027, USA <sup>3</sup>Department of Oncological Sciences and Huntsman Cancer Institute, Howard Hughes Medical Institute, University of Utah School of Medicine, Salt Lake City, UT 84112, USA <sup>4</sup>Department of Pediatrics, University of California, San Francisco, CA, 94143, USA <sup>5</sup>Lunenfeld-Tanenbaum Research Institute, University of Toronto, ON, M5G1X5, Canada <sup>6</sup>Department of Molecular Genetics, University of Toronto, ON, M5S1A8, Canada

\*Correspondence address. Department of Obstetrics, Gynecology and Reproductive Sciences, University of California, 513 Parnassus Ave, HSW San Francisco, CA, 94143, USA. E-mail: paolo.rinaudo@ucsf.edu  <https://orcid.org/0000-0002-6528-6009>

Submitted on June 29, 2020; resubmitted on September 10, 2020; editorial decision on September 18, 2020

**ABSTRACT:** The preimplantation stage of development is exquisitely sensitive to environmental stresses, and changes occurring during this developmental phase may have long-term health effects. Animal studies indicate that IVF offspring display metabolic alterations, including hypertension, glucose intolerance and cardiac hypertrophy, often in a sexual dimorphic fashion. The detailed nature of epigenetic changes following *in-vitro* culture is, however, unknown. This study was performed to evaluate the epigenetic (using whole-genome bisulfite sequencing (WGBS) and assay for transposase-accessible chromatin using sequencing (ATAC-seq)) and transcriptomic changes (using RNA-seq) occurring in the inner cell mass (ICM) of male or female mouse embryos generated *in vivo* or by IVF. We found that the ICM of IVF embryos, compared to the *in-vivo* ICM, differed in 3% of differentially methylated regions (DMRs), of which 0.1% were located on CpG islands. ATAC-seq revealed that 293 regions were more accessible and 101 were less accessible in IVF embryos, while RNA-seq revealed that 21 genes were differentially regulated in IVF embryos. Functional enrichment analysis revealed that stress signalling (STAT and NF- $\kappa$ B signalling), developmental processes and cardiac hypertrophy signalling showed consistent changes in WGBS and ATAC-seq platforms. In contrast, male and female embryos showed minimal changes. Male ICM had an increased number of significantly hyper-methylated DMRs, while only 27 regions showed different chromatin accessibility and only one gene was differentially expressed. In summary, this study provides the first comprehensive analysis of DNA methylation, chromatin accessibility and RNA expression changes induced by IVF in male and female ICMs. This dataset can be of value to all researchers interested in the developmental origin of health and disease (DOHaD) hypothesis and might lead to a better understanding of how early embryonic manipulation may affect adult health.

**Key words:** IVF / DOHaD / epigenetics / in-vitro culture / preimplantation embryo

## Introduction

ARTs are widely used, and as of today more than 8 million children, or 1.7% of the population in the Western world, have been conceived with the technology (Luke, 2017). The procedures are effective and safe; however, there are concerns regarding their long-term health consequences (Servick, 2014). These concerns arise from the fact that during specific windows of development, the organism is sensitive to external cues. As stated by the developmental origin of health and disease (DOHaD) hypothesis, if the environment is suboptimal, the

individual can survive the stressful event, but it is predisposed to adult-onset diseases, like hypertension, diabetes or stroke (Barker and Osmond, 1986). In this regard, the Dutch Famine cohort study provided evidence of the impact of nutrient deprivation during different times of pregnancy on adult offspring health (Heijmans *et al.*, 2008).

The preimplantation stage of development is exquisitely sensitive to environmental stresses, and changes occurring during this developmental phase may have long-term health effects. For example, culturing embryo *in vitro*, as done with ARTs, is associated with alteration in offspring growth. We and others have shown that mouse offspring

following IVF are predisposed to changes in embryo growth with alteration of the blastocyst transcriptome (Feuer *et al.*, 2017), foetal and placental growth (Delle Piane *et al.*, 2010; Bloise *et al.*, 2012), and postnatal growth, with metabolic alterations (Donjacour *et al.*, 2014; Feuer *et al.*, 2014b), hypertension (Rexhaj *et al.*, 2013), cardiac hypertrophy (Donjacour *et al.*, 2014) or behavioural changes (Ecker *et al.*, 2004; Fernandez-Gonzalez *et al.*, 2004). In addition, in the bovine model, multiple studies have shown that IVF is correlated to congenital malformations, perinatal mortality and alteration of postnatal health (van Wagtenonk-de Leeuw *et al.*, 1998; Boerjan *et al.*, 2000). In humans, ARTs have been associated with an increased risk of birth defects (increases of nearly 30%, (Boulet *et al.*, 2016)), premature birth (odds ratio (OR) 2.0), very low birth weight (OR 2.7 (Jackson *et al.*, 2004)) and perinatal complications (Bosch and Sutcliffe, 2017). Furthermore, while postnatal data are limited and non-conclusive, offspring generated by IVF have shown an increased incidence of glucose intolerance, hypertension and cardiac hypertrophy in both mice and humans (Rexhaj *et al.*, 2011; Donjacour *et al.*, 2014; Guo *et al.*, 2017; Meister *et al.*, 2018).

The most likely molecular mechanisms explaining such long-term effects are epigenetic changes. Indeed, the preimplantation embryo undergoes demethylation starting at syngamy and reaching the lowest level of methylation at the blastocyst stage (29% methylation (Guo *et al.*, 2014)). Recent findings suggest an intricate relationship between demethylation, *de novo* methylation and methylation maintenance during methylation reprogramming (Canovas *et al.*, 2017). Histone modifications also interact with DNA methylation for epigenetic regulation (Shi and Wu, 2009). During embryo development, histone modifications undergo dynamic changes, and each stage of development results in stage-specific alterations (Shi and Wu, 2009; Xu and Xie, 2018). Recent literature has noted that extensive changes in chromatin accessibility occur pre- and post-zygotic genome activation; these changes appear to be conserved between mice and humans (Wu *et al.*, 2018).

Interestingly numerous imprinting disorders have been correlated with ARTs, including Angelman syndrome, Beckwith-Wiedemann syndrome and Silver-Russell syndrome (Melamed *et al.*, 2015; Canovas *et al.*, 2017). White *et al.* (2015) showed that ART generated human preimplantation embryos possess a high frequency of imprinted methylation errors, which confirms the vulnerability of the embryo to *in-vitro* manipulation and environmental stressors. Animal studies have shown that *in-vitro* culture alters global DNA methylation patterns (Shi and Haaf, 2002); importantly, suboptimal culture conditions were found to induce more severe DNA methylation changes at imprinted loci than optimal culture conditions (Doherty *et al.*, 2000), suggesting a dose-response effect. Furthermore, studies using yellow agouti viable (A<sup>vy</sup>) mice, one of the best characterised epigenetic animal models to date (Jirtle, 2014), have shown that embryo *in-vitro* culture results in decrease in intracisternal A-particle (IAP) methylation in offspring (and therefore in increase of yellow mice) compared to natural mating (Morgan *et al.*, 2008), indicating that embryo culture might have significant effects on the epigenome of embryos and offspring.

In summary, a significant body of evidence indicates an important sensitivity of the preimplantation embryo to epigenetic remodelling (Guo *et al.*, 2014). It remains to be elucidated if the epigenetic alterations in the early embryo may predispose the individual to adult diseases (Hon *et al.*, 2013).

Another critical factor to consider is that epigenetic marks might have an asymmetrical distribution between male and female embryos (Bermejo-Alvarez *et al.*, 2011; Canovas *et al.*, 2017). Gene expression studies indicate that approximately 50 genes are differentially expressed more than 2-fold between male and female bovine blastocysts (Bermejo-Alvarez *et al.*, 2010). Furthermore, Tan *et al.* (2016) showed that IVF foetuses had a higher male to female sex ratio, and overall female IVF embryos had a higher apoptosis rate, secondary to the dysregulation of X-linked genes, *Xist*, *Hprt* and *Pgkl*. The dysregulation of the X-linked genes in female embryos following IVF suggests that some loci might show sex-specific epigenetic alterations (Tan *et al.*, 2016).

Furthermore, in prior studies, we have found a sexually dimorphic effect of IVF on mouse growth (Donjacour *et al.*, 2014; Feuer *et al.*, 2014a). For example, in inbred mice, we found that only females develop increased weight gain and mild glucose intolerance with age (Feuer *et al.*, 2014b), strongly suggesting a sex-dependent sensitivity of the embryo to the environmental conditions experienced by the embryo during the process of IVF and embryo culture. It is, therefore, possible that male and female embryos are physiologically primed to differentially respond to environmental changes in a sex-specific fashion (Feuer *et al.*, 2014a).

The primary objective of this work was to understand whether preimplantation embryo manipulation is associated with DNA methylation and histone changes in a sex-dependent fashion. Given that blastocysts contain two different tissues (inner cell mass (ICM) and trophectoderm (TE)) and given that the ICM will give rise to the embryo proper, we decided to focus our analysis on the ICM only. To do so, we compared DNA methylation using whole-genome bisulfite sequencing (WGBS) (Meissner *et al.*, 2005; Gu *et al.*, 2011; Urich *et al.*, 2015), chromatin accessibility, using Assay for transposase-accessible chromatin using sequencing (ATAC-seq) (Buenrostro *et al.*, 2015), and gene expression using RNA-sequencing (RNA-seq) (Hrdlickova *et al.*, 2017) in the ICM of male and female mouse blastocysts conceived *in vivo* or *in vitro*.

## Materials and methods

### IVF and embryo culture

Embryos produced *in vivo* and *in vitro* were isolated from superovulated dams. CF-1 outbred female mice (6–9 weeks old) were injected with 5 IU Pregnant Mare Serum Gonadotropin (PMSG; Biovendor, RPI782725000) and 46–48 h later with 5 IU hCG (Sigma-Aldrich, CG5). On average, we obtained 25 oocytes per mouse. For the group of the oocytes fertilised *in vitro*, oocytes were obtained the morning after the hCG injection from the ampullae and incubated in potassium simplex optimised medium with amino acids (KSOM + AA; Millipore, MR-106-D) and the sperm obtained from the cauda epididymis of outbred male B6D2F1/J mice for 4 h. Presumptive zygotes were washed and cultured in KSOM medium to the stage of expanded blastocyst under 5% O<sub>2</sub>, 5% CO<sub>2</sub>, 90% nitrogen at 37°C. On average, the fertilisation rate was 54% and the blastocyst development rate was 71%. *In-vivo* expanded blastocysts were flushed out of the uterus (FB for flushed blastocysts) of the mice 94–96 h post-hCG injection and mating. ICM and TE cells were then held in KSOM medium, ready

to be separated from each other via immunosurgery. In total, we used 293 female and 61 male mice. Only expanded blastocysts of similar morphology in both IVF or FB groups were used to isolate ICM.

### Separation of TE cells from ICM: immunosurgery

Separation of the ICM and the TE cells for future analyses was achieved with immunosurgery (Solter and Knowles, 1975). In total, we performed 21 IVF and 19 FB replicates. Of the obtained 305 blastocysts, 196 were subjected to immunosurgery and sexed.

The blastocysts were washed in KSOM medium, and the zona pellucida was removed using Tyrode's solution (Sigma, T1788). Blastocysts were then incubated in 10% anti-mouse rabbit antibody (Sigma, M5774) solution for 30 min. After incubation, blastocysts were washed in KSOM medium and were then incubated for 30 min in 25% guinea pig complement serum (Sigma, S1639) solution. As soon as the TE lysis started, intact TE cells were rapidly removed and stored for subsequent sexing. Each pair of ICM and TE cells was given a unique code that could permit exact identification of its origin. The ICM samples were then cleaned from the TE cells by repeatedly pipetting up and down. ICM and TE cells were rinsed multiple times in KSOM medium to remove any traces of complement. To ensure there was no TE still attached to the ICM after immunosurgery, representative ICM was stained with Fluoresbrite YG Microspheres (Polysciences, 17154-10) according to the protocol (Szczipanska et al., 2011) and visualised under a fluorescent microscope to determine their purity (Supplementary Fig. S1). Intact blastocysts were used as a control. For WGBS, ICM was placed in KSOM medium and stored at  $-80^{\circ}\text{C}$ . For ATAC-seq, only ICM was utilised and were immediately placed in lysis buffer to begin the protocol described below. For RNA-seq, ICM was immediately placed individually in lysis buffer provided by LC Sciences and stored at  $-80^{\circ}\text{C}$ ; TE cells were immediately processed for embryo sex determination (described in the next section).

### DNA isolation from TE cells

Genomic DNA was isolated from the TE cells to determine the sex of the correspondent ICM. Isolation was performed using the Arcturus PicoPure DNA Extraction Kit (Thermo Fisher Scientific, KIT0204) according to the manufacturer's protocol. TE cells were incubated at  $65^{\circ}\text{C}$  with reconstitution buffer and proteinase K for 3 h, followed by  $95^{\circ}\text{C}$  for 10 min to inactivate the proteinase K. Isolated DNA samples were then used to determine the sex of the blastocyst.

### Sex determination of the TE cells

After DNA isolation from the TE cells, quantitative real-time PCR was completed following the modified protocol from Prantner et al. (2016). The genes used for sex determination of the TE cells were X-chromosome gene lysine-specific demethylase 5 (Kdm5c) and the corresponding Y-chromosome gene (Kdm5d). The sizes of the fragments from the X and Y chromosomes (331 and 302 bp, respectively) resulted in distinguishable melting curves. If one melt curve was present, the sample was deemed a female, and if there were two, it was a male. After the determination of the sex of the TE cells, ICM was classified based upon the sex. The sex ratio following IVF was 52%

females and 48% males. The sex ratio in FB was 42% females 58% males.

### Whole-genome bisulfite sequencing

Four groups (IVF male, IVF female, FB male and FB female), each resulting from pooling 15 ICM, were used. Since we expected that each ICM would contain a minimum of 10 cells (Giritharan et al., 2007) and since WGBS requires a minimum of 100 cells, we decided to pool 15 ICMs to obtain a sufficient number of cells to provide reliable technical results. WGBS was completed using the Methyl-MaxiSeq platform from Zymo Research (Denomme et al., 2018). Pooled ICMs of IVF and FB blastocysts were provided to Zymo for library preparation using the Pico Methyl-Seq library preparation kit (Zymo). Libraries for Methyl-MaxiSeq were prepared directly from the ICM without any additional extraction. Due to the low DNA input from ICM, the Pico Methyl-Seq library preparation kit was used (Zymo, Catalog #D5455). The DNA was subjected to bisulphite conversion using the EZ DNA Methylation-Lightning kit (Zymo, Catalogue #D5020). Briefly, the lightning reagent was mixed with the genomic DNA and incubated at  $98^{\circ}\text{C}$  for 8 min, and 1 h at  $54^{\circ}\text{C}$ . Samples were subjected to a column, incubated with L-disulphonation buffer, and washed M-wash buffer. Bisulphite-converted DNA was then eluted from the columns. After bisulphite conversion, samples were incubated with a PreAmp primer and polymerase. After the PreAmp polymerase reaction, samples were transferred to a Zymo-Spin IC column to be purified and concentrated using the DNA Clean & Concentrator-5 (Zymo, Catalogue #D4003). After purification, samples were subjected to PCR to amplify the library for five cycles using the following PCR conditions:  $94^{\circ}\text{C}$  for 30 s; thermocycling at  $94^{\circ}\text{C}$  for 30 s,  $45^{\circ}\text{C}$  for 30 s and  $55^{\circ}\text{C}$  for 30 s; followed by  $68^{\circ}\text{C}$  for 5 min. Following amplification, libraries were purified again using the Zymo-Spin IC column and eluted. Individual libraries were prepared with unique Illumina Index primers. The library was mixed with LibraryAmp master mix and the designated index primer. Samples were subjected to PCR amplification for a total of 10 cycles using the following conditions:  $94^{\circ}\text{C}$  for 30 s; thermocycling at  $94^{\circ}\text{C}$  for 30 s,  $58^{\circ}\text{C}$  for 30 s and  $68^{\circ}\text{C}$  for 1 min; followed by  $68^{\circ}\text{C}$  for 5 min. The final product was purified using the Zymo-Spin IC column and eluted. Library fragment size and concentration was evaluated using the Agilent 2200 TapeStation instrument and sequenced on the Illumina HiSeq 2500 platform.

### Assay for transposase-accessible chromatin using sequencing

Individual ICM (IVF male  $n = 18$  replicates, IVF female  $n = 18$ , FB male  $n = 7$  and FB female  $n = 12$ ) was examined by ATAC-seq. The protocol used for the project was modified from Wu et al. (2016). Briefly, samples were lysed in lysis buffer (10 mM Tris-HCl (pH 7.4), 3 mM  $\text{MgCl}_2$ , and NP-40) for 15 min on ice to prepare the nuclei. Immediately after lysis, nuclei were spun at 500g for 5 min to remove the supernatant. Nuclei were then incubated with the Tn5 transposome and tagmentation buffer at  $37^{\circ}\text{C}$  for 30 min (Nextera). After the tagmentation, the stop buffer was added directly into the reaction to end the tagmentation. PCR was performed to amplify the library for 15 cycles using the following PCR conditions:  $72^{\circ}\text{C}$  for 5 min; thermocycling at  $95^{\circ}\text{C}$  for 30 s and  $72^{\circ}\text{C}$  for 90 s; followed by  $72^{\circ}\text{C}$  10 min.

Mitochondrial depletion was performed. Briefly, the NGG protospacer adjacent motif (PAM) sequences were first identified in the genome of mitochondria, and the upstream 20 bp of PAM sequences were used as sgRNA candidates. A total of 114 sgRNAs were then selected and synthesised to cover approximately every 140 bp over the mitochondrial genome. Paired oligonucleotides were annealed, pooled and were ligated to the pUC57kan-T7-gRNA vector, which was further transformed and amplified. *In-vitro* transcription was performed to produce sgRNAs (MEGAscript<sup>TM</sup> Kit, Thermo Fisher Scientific). Each ATAC-seq library was incubated with 330–500 ng sgRNA and 1 µg Cas9 protein (PNA Bio CP01-50) for 2 h at 37°C. After incubation, the reaction was treated by RNase A before being terminated by adding the stop buffer (30% glycerol, 1.2% SDS, 250 mM EDTA, pH 8.0). The ATAC-seq library was further purified by 1.2× AMPure beads. The reaction was incubated with the beads for 15 min. The beads were washed with 80% EtOH, and then elution buffer was added. The supernatant was measured for absorbency with Qbit DNA HS Assay (Thermo Fisher Scientific). Fragment sizes were analysed using 5% TBE-polyacrylamide gel electrophoresis, and samples were subjected to sequencing on HiSeq 2500 (Illumina) according to the manufacturer's instruction.

Sex of the ICMs was determined in a three-step method using the Male Sex Region on the Y Chromosome (MSY). After ATAC-seq reads were aligned, all alignments that overlapped an annotated repeat on the Y-chromosome were discarded because these repeats are also found on the X-chromosome. The next step was to look at the distribution of the %Y chromosome reads, which were bimodal in male samples. If samples were still unclear, reads were removed that aligned to the Y-chromosome PAR (pseudautosomal region), and only non-repetitive MSY reads were considered.

## RNA-sequencing

Three independent biological replicates of individual blastocysts (IVF male, IVF female, FB male and FB female) were analysed. After immunosurgery, individual ICM was placed in a proprietary lysis buffer with RNase E provided by LC Sciences (Houston, TX). Sequencing libraries were generated by LC Sciences using Poly(A)-tail selection for mRNA. Briefly, lysed samples were incubated with poly-T oligos attached to magnetic beads to isolate the poly(A) mRNA. Samples were then purified. After purification, the mRNA poly(A) samples were fragmented into small pieces using divalent cations at elevated temperatures. The cleaved fragments underwent reverse transcription to form cDNA. Samples then underwent second strand synthesis with a strand-specific library preparation by the dUTP method. This method incorporated dUTP into the second strand of cDNA for directionality identification (Hrdlickova *et al.*, 2017). Barcoded adapters for sample identification were ligated to the individual samples. Libraries then underwent uracil-DNA glycosylase (UDG) treatment to degrade the second strand containing the dUTP, enabling only the first strand to be amplified via PCR (Hrdlickova *et al.*, 2017). Sequencing was performed using an Illumina HiSeq platform with 150 base pair, paired-end reads.

## Bioinformatics and statistical analyses

For IVF versus FB comparison, FB was considered the control, while for Male versus Female, the control comparison was the Female.

## Whole-genome bisulfite sequencing

The ends of the raw fastq reads were trimmed at positions with a quality score of <30 using Fastq-mcf (Aronesty, 2011). The trimmed reads were aligned to the mouse genome build, mm9, using the bismark aligner (Krueger and Andrews, 2011) that uses bowtie2 (Langmead and Salzberg, 2012) with the following options: non\_directional score\_min L, 0,-0.4. The aligned reads were deduplicated using deduplicate\_bismark (Krueger and Andrews, 2011). The genome-wide methylation levels were extracted using the bismark\_methylation\_extractor (Krueger and Andrews, 2011). For WGBS, the mapping efficiency of our samples was 44%. IVF samples had  $1.50 \times 10^9$  reads after filtering for quality, and  $6.49 \times 10^8$  reads mapped to the mouse genome. FB samples resulted in  $1.48 \times 10^9$  reads after filtering for quality, and  $6.64 \times 10^8$  reads mapped to the mouse genome.

The differentially methylated regions (DMRs) for IVF versus FB and Male versus Female were identified using the bseq package (Hansen *et al.*, 2012) in R. The ns (the minimum number of methylation loci in a smoothing window) and h (the minimum number of bases in the smoothing window) parameters that are part of the BSmooth function were set at 70 and 1000, respectively. The computation of variance in BSmooth.tstat was assumed to be paired either by gender for the IVF versus FB comparison or by fertilisation status for the Male versus Female comparison. Regions were identified as DMR either if they were in the bottom or the top 2.5% quantiles of the resulting t-statistics using the dmrfinder function. These regions were further filtered if the absolute value MaxStat parameter from the output of this function is  $\geq 3.0$ . Significance was denoted as  $P \leq 0.003$ . The annotations for the DMRs were assessed using the annotatr (Cavalcante and Sartor, 2017) R package.

Once DMR were determined, Genomic Regions for Enrichment Analysis Tool (GREAT version 4.0.4, <http://great.stanford.edu>) was used to associate genes to the regions (McLean *et al.*, 2010). The functional enrichment analysis was performed using g:Profiler<sup>β</sup> (version e99\_eg46\_p14\_55317af) with g:SCS multiple testing correction method applying a significance threshold of *P*-adjusted value <0.05 (<https://biit.cs.ut.ee/gprofiler/gost>), (Raudvere *et al.*, 2019) uploading the list of genes within DMRs. The overrepresented biological processes (BPs) or molecular functions (MFs) were summarised with REVIGO (reduce + visualise Gene Ontology, <http://revigo.irb.hr>) to avoid redundant gene ontology (GO) terms (Supek *et al.*, 2011). The nomenclature of BPs and MFs uses terms of the Gene Ontology Consortium (Ashburner *et al.*, 2000). The transcription factor binding site predictions were identified using the TRANSFAC database (Matys *et al.*, 2006) as part of the functional enrichment analysis provided by g:Profiler<sup>β</sup>. The statistically significant canonical pathways [CPs, *P*-value < 0.05, using the right-tailed Fisher's exact test] were identified using Ingenuity<sup>®</sup> Pathway Analysis (IPA<sup>®</sup>, <http://ingenuity.com>).

For long repetitive element and CpG island analyses, the annotated regions associated with repeat elements and the CpG islands for the mouse genome build mm9 was downloaded from the UCSC Genome Browser (Karolchik *et al.*, 2004, 2012) (<http://genome.ucsc.edu>). The average methylation level for each of the four samples in each of the annotated regions was computed using the bedmap program that used the coverage file produced from the bismark\_methylation\_extractor program (Krueger and Andrews, 2011) and the annotated regions as a bed file. Paired *t*-tests were used to determine differentially

methylated repeat elements and CpG islands for the IVF versus FB, and the Male versus Female comparison and significance was denoted as  $P$ -value  $< 0.05$ . The imprinted genes within the DMRs were identified using the atlas of imprinting for mouse developmental stages and tissues (Babak et al., 2015).

## Assay for transposase-accessible chromatin using sequencing

The raw sequence data in fastq files were aligned to the mouse genome build mm9 using bowtie2 aligner (Langmead and Salzberg, 2012). Duplicate reads from the aligned bam files were removed using the Picard MarkDuplicates program (<http://broadinstitute.github.io/picard>). Open chromatin regions for each sample were called using the narrowPeak output of the MACS2 peak caller (Zhang et al., 2008). A consensus set of peaks was determined across replicates using the—everything followed by—merge options of the bedops program (Neph et al., 2012). A peak was included in the consensus set if it included a peak called by MACS2 for at least one of the replicates. The number of reads mapping to each of the consensus regions for each of the replicates was determined using the subread featureCounts program (Liao et al., 2013, 2014), which created a matrix of raw counts: the number of rows equals the number of consensus regions, and the number of columns equals the number of samples. Regions that did not have at least five reads in at least five of the samples were filtered out. The raw counts matrix was then normalised using the edgeR bioconductor R package (Robinson et al., 2010; McCarthy et al., 2012). A linear model was fit for the mean normalised signal in each of the filtered consensus regions (Ritchie et al., 2015). This method is specially designed for analysing complex experiments with a variety of experimental conditions and predictors. This model allowed for the main effects of IVF versus FB and Male versus Female. The significance of the regions associated with IVF was estimated using the edgeR package by testing the null hypothesis that the main effect of IVF is equal to zero. Similarly, the significance of the regions associated with Male was estimated using the edgeR package by testing the null hypothesis that the main effect of Male is equal to zero. Significance was denoted as a false discovery rate (FDR)  $< 0.05$ . Once differential regions were determined, GREAT was used to associate genes to the regions. g: Profiler<sup>β</sup> was used to determine enriched BPs ( $P$ -adjusted value  $< 0.05$ ) that were summarised by REVIGO. The statistically significant CPs ( $P$ -value  $< 0.05$ ) were identified using IPA<sup>®</sup>.

### RNA-sequencing

Overall, the mapping efficiency of our samples was 70%. After sequencing, trimming of known adapters and low-quality regions of reads was performed using Fastq-mcf (Aronesty, 2011). Sequence quality was assessed using the programs FastQC and RSeQC (Andrews, 2010; Wang et al., 2012). STAR was used to align the reads to the mouse reference genome mm9 (Dobin et al., 2013). Reads were assigned to genes using FeatureCounts in the Subread suite using the Ensembl gene annotation. Differential expression was determined using edgeR (Robinson et al., 2010). Genes with reliable exon coverage based on the UCSC Genome Browser tracks were considered differentially expressed (DEG) if  $|\text{fold change}| > 2$  and  $\text{FDR} < 0.05$ . The functional enrichment analysis was done with g: Profiler<sup>β</sup> to identify the overrepresented GO terms ( $P$ -adjusted value  $< 0.05$ ) using the list

of DEG. The statistically significant CPs ( $P$ -value  $< 0.05$ ) were identified using IPA<sup>®</sup>.

### Overlap between WGBS, ATAC-Seq and RNA-Seq

Venn diagrams (<https://bioinformatics.psb.ugent.be/webtools/Venn>) were created combining gene lists of each of the three next-generation sequencing (NGS) platforms (WGBS, ATAC-Seq and RNA-seq). To evaluate for variance among samples, the coefficient of variation (CV) was calculated and compared.

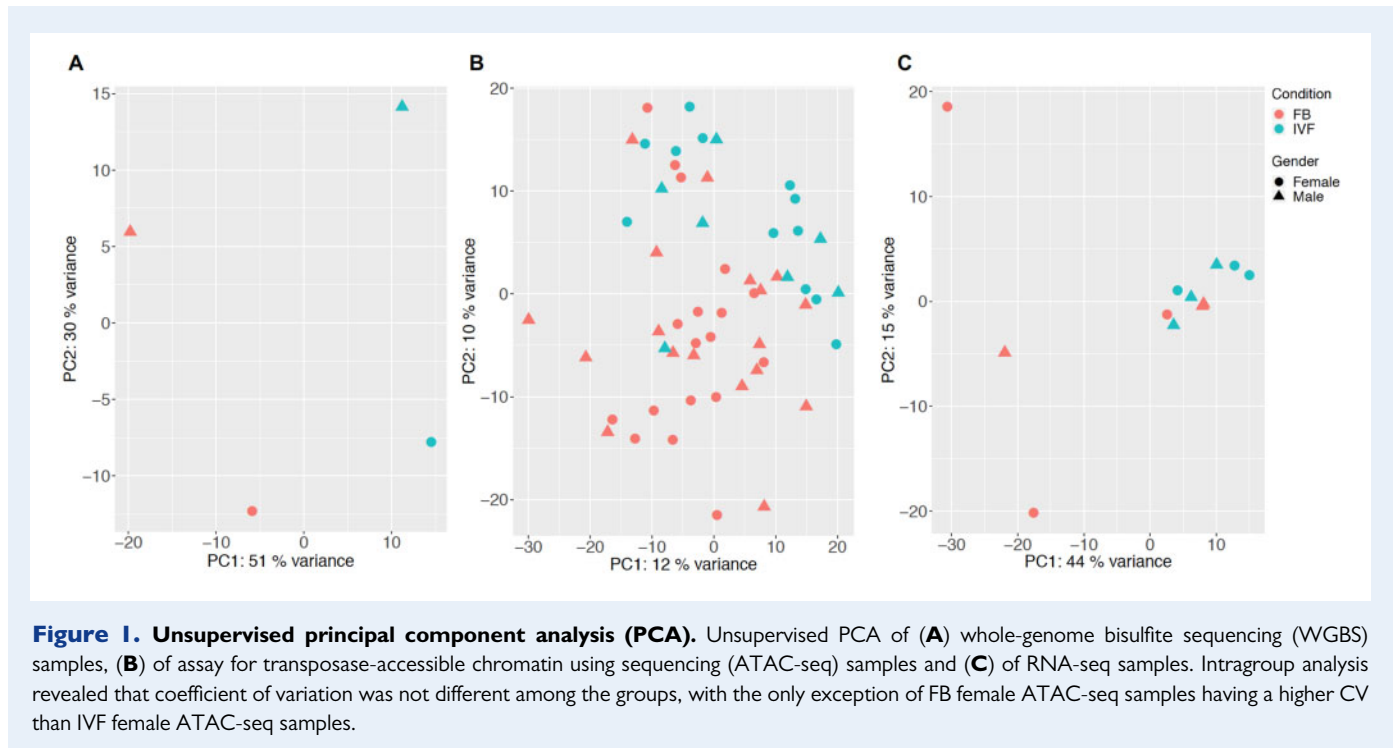
## Results

### ICM of embryos generated by IVF show an increase in hyper-methylated DMR distributed throughout the genome but not in proximity to transcription start sites

Unsupervised principal component analysis shows that IVF and FB samples cluster as independent groups (Fig. 1A). Overall, only 3% of DMR ( $n = 1624$ ) were statistically different between IVF and *in-vivo* generated ICM (Fig. 2A). Since 85% of DMRs contained the regulatory elements of two different genes (Supplementary Fig. S2A), we identified 1648 genes in the hyper-methylated DMR and 626 in proximity to hypo-methylated DMR while 146 genes were located in DMR with both evidence of hyper- and hypo-methylation (Supplementary File S1A). Out of the total DMR identified (1624), the majority ( $n = 1156$ , i.e. more than two-thirds) were hyper-methylated in IVF samples. DMRs appeared to be equally distributed across all chromosomes, with no evidence of clustering (Supplementary Fig. S3A). They were more frequently located 50–500 kb distal to the transcription start sites (Supplementary Fig. S2B), particularly in intronic and intergenic regions (Fig. 2A). Surprisingly, only 0.17% of CpG islands were differentially methylated between IVF and control embryos, and only a few DMR were located on known gene promoters ( $n = 49$ ) or enhancers ( $n = 60$ ; Supplementary File S1B). Although seven imprinted genes showed areas of differential methylation, only *Plagl1* showed methylation changes with closely spaced ZFBS-Morph overlap, suggesting regulation on the imprinting control region (ICR, Supplementary File S1C) (Bina, 2017). Transposable elements (LINE, SINE and LTR) were not differentially methylated (data not shown). In addition, mitochondrial DNA (mtDNA) methylation appeared not to be different among the groups.

### DMRs in ICM of IVF embryos are enriched for genes involved in developmental and cellular metabolic process, as well as in the regulation of signalling and gene expression

Functional enrichment analysis showed that BPs overrepresented included developmental process, regulation of cellular and BPs, biogenesis, cellular metabolic process and regulation of signalling (Supplementary File S1D). A sub-analysis in enhancers or promoters regions identified few putative transcription-binding sites for transcription factors (Supplementary File S1E) involved in chromatin



remodelling (CTCF), differentiation of insulin-producing beta cells (Pax4) and development (AP-2 alpha, FOXN4, WTI).

### Chromatin accessibility analysis revealed that the ICM of IVF embryos have more accessible areas than control embryos, affecting genes involved in developmental process

Unsupervised principal component analysis showed that although the majority of control samples tended to co-localise, there was overlap between groups, suggesting that differences between groups were minimal (Fig. 1B). Analysis of variation among samples revealed that only one comparison, FB female (CV = 13.69%) versus IVF female (CV = 4.62) was statistically different ( $P=0.02$ ) with FB females showing higher variation.

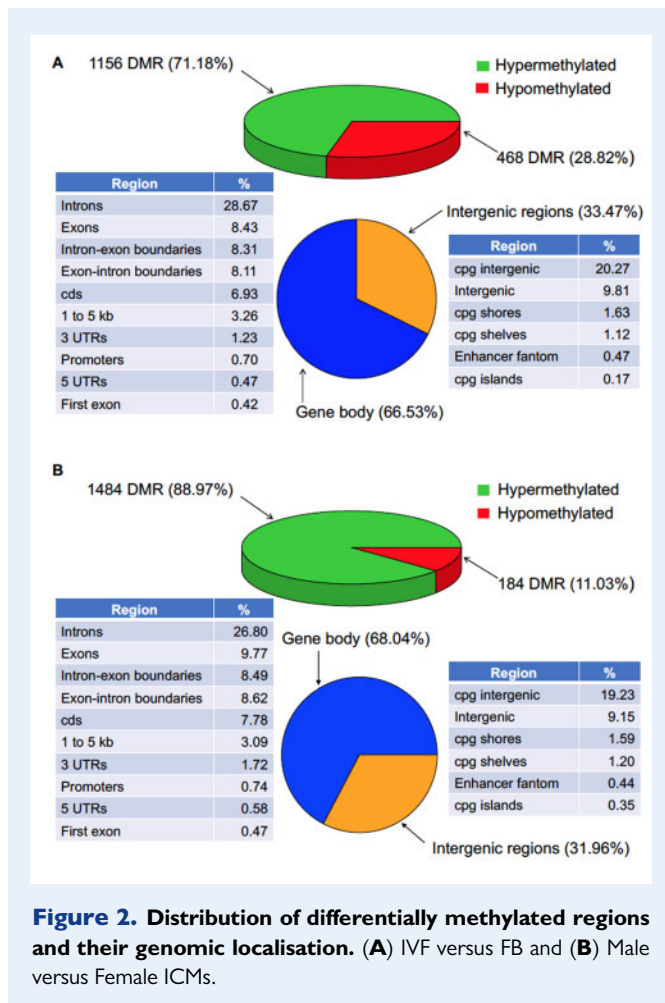
ICM of IVF embryos had 394 regions (FDR < 0.05;  $n=619$  genes) with different chromatin accessibility. In particular, 293 regions ( $n=457$  genes) were more accessible, and 101 regions ( $n=162$  genes) less accessible compared to ICM of control embryos (Supplementary File S2A). Morphogenesis, developmental process and cell–cell adhesion were the main non-redundant BPs overrepresented (Supplementary File S2B). Among transcription factors binding to areas of open chromatin kaiso (Supplementary File S2C) showed the highest statistical significance.

### There are minimal transcriptomic differences in ICM of IVF embryos

FB and IVF samples did not cluster together, indicating minimal transcriptomic differences (Fig. 1C). ICM of IVF embryos differed in expression of 21 genes (11 up- and 10 down-regulated, Supplementary File S3A) and only two CPs (threonine degradation and the role of Oct4 in mammalian embryonic stem cell pluripotency) were identified (Supplementary File S3B).

### Genes involved in development and regulatory processes, as well as cardiac hypertrophy, show epigenetic differences in ICM of IVF embryos

While several BPs and CPs were uniquely identified in WGBS and ATAC-seq platforms (WGBS see Supplementary File S1 and ATAC-seq: Supplementary File S2), we found 35 CPs changed in both platforms, highlighting cardiac hypertrophy signalling (enhanced) in the top 10 of both NGS platforms (Fig. 3). The functional enrichment analysis using the list of 131 common genes identified by WGBS and ATAC-seq (Supplementary File S4A) showed two MFs (RNA polymerase II regulatory region and transcription factor activity: Supplementary File S4B) and 14 CPs (highlighting, STAT3 and mammalian embryonic stem cell pluripotency, Supplementary File S4D) overrepresented. Four transcription factors showed evidence of epigenetic regulation (E2F, Kaiso, BEN, and FOXN4, Supplementary File S4C). No common genes were identified between WGBS, ATAC-seq and RNA-seq (Fig. 4).



## The effect of sex: ICM of male embryos has an increase in DNA methylation and at loci involved in developmental process

All platforms showed minimal clustering of samples based on sex (Fig. 1). Overall only 2.6% of DMR were statistically different between male and female embryos and were distributed across all chromosomes (Supplementary Fig. S3B). Male embryos showed an increase in methylation in numerous DMRs (88.97%), compared to female embryos; we identified 2127 genes in the hyper-methylated DMR, 230 were in proximity to hypo-methylated DMR, while 81 genes were located in DMR with both evidence of hyper- and hypo-methylation (Supplementary File S5A). The majority of DMRs were located 50–500 kb distally to the transcription start sites, equivalent to a third of the genes identified (Supplementary Fig. S2C and D), and the highest frequency of DMRs was in intronic and intergenic regions (Supplementary Fig. S2B). Only 51 promoters and 58 enhancers were located within DMRs (Supplementary File S5B). Although nine imprinted genes were differentially methylated, only *Peg3* had methylation changes in the ICR (Supplementary File S5C). BPs that were overrepresented

included developmental process, regulation of transcription from RNA polymerase II promoter and metabolic process (Supplementary File S5D). CPs identified included TGF- $\beta$  signalling, mouse embryonic stem cell pluripotency, role of NFAT in cardiac hypertrophy, adipogenesis pathway and cardiac hypertrophy signalling (enhanced).

## There are few loci with different chromatin accessibility and only one gene with different expression in ICM of male versus female embryos

There were only 22 regions (12 genes) with different chromatin accessibility between male and female FB embryos and 28 regions (15 genes) between male and female IVF embryos (Supplementary File S6A and S6C, respectively). The CPs allograft rejection, OX40 and *Cdc42* signalling were identified in both contrasts (Supplementary File S6B and S6D). The ribosomal gene *Rps3a3* was differentially expressed in FB male versus FB female contrast. There were no common genes or CPs changed in all three platforms in ICM of male versus female embryos.

## Discussion

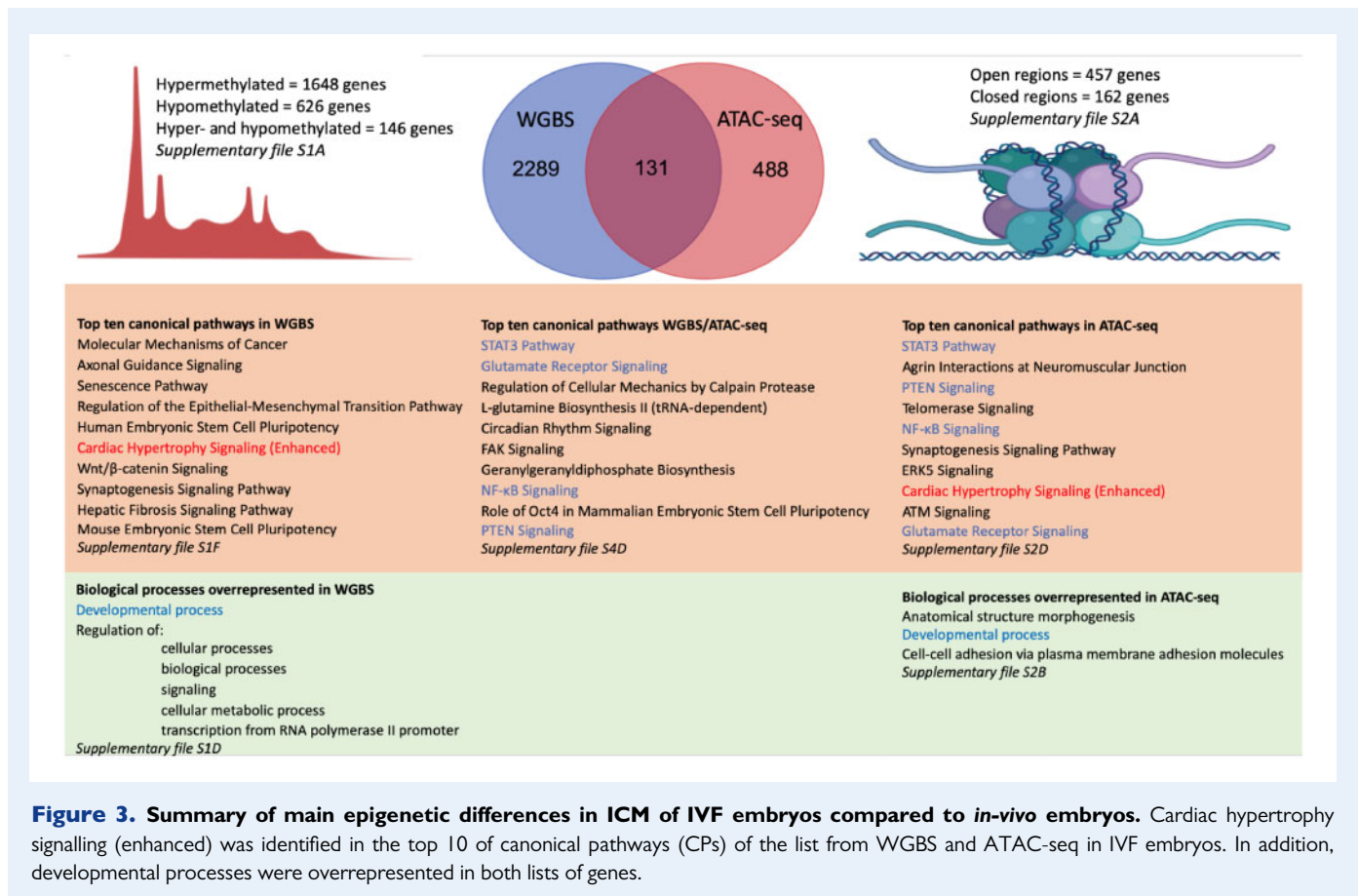
This study provides the first description of global DNA methylation, histone and transcriptomic changes that occur in the ICM mouse embryos following IVF and embryo culture. Given the known sexual dimorphic effect of *in-vitro* culture (Bermejo-Alvarez et al., 2011), we further analysed if male and female embryos respond differently to the IVF process. The large data set generated in this study will have wide relevance to the many scientists interested in the DOHaD field and might help elucidate the epigenetic origin of adult health (Servick, 2014).

Overall, when comparing the epigenetic profile of IVF versus control ICM, there are several notable findings. First, the correspondence between platforms was relatively low. For example, of the differentially methylated genes, only 5% (131/2420) were located in an area with abnormal chromatin structure (Fig. 4).

Second, WGBS and ATAC-seq platforms identified some common changes when comparing ICM of IVF versus *in-vivo* embryos. While we are not surprised that developmental and regulatory BPs might be differentially regulated in embryos cultured *in vitro*, it is highly relevant that the CP cardiac hypertrophy (enhanced) was identified in ICM of IVF mice. In fact, both mice (Donjacour et al., 2014) and children (Zhou et al., 2014; Valenzuela-Alcaraz et al., 2019) generated by IVF have shown evidence of increased left ventricular thickness. While abnormalities in placentation are known to induce alteration in cardiac development (Thornburg et al., 2010), the findings of epigenetic changes in the ICM of IVF embryos suggest that cardiac development could be controlled by metabolic and energetic cues sensed in the early embryo.

WGBS and ATAC-seq also identified genes associated with stress in IVF embryos. WGBS functional enrichment analysis identified the BP cellular response to stress (Supplementary File S1D) and the CPs IL-23 signalling and Th1/Th2 activation pathway (Supplementary





File S1F). Similarly, ATAC-seq showed that 4 of the top 10 CPs (STAT3, NF- $\kappa$ B, ERK5 and ATM signalling; Supplementary File S2D) were modified. While it is well described that IVF embryos show transcriptomic (Feuer *et al.*, 2017) and mitochondrial (Belli *et al.*, 2019) evidence of stress, this is the first report indicating that IVF embryos also have epigenetic evidence of stress.

Among genes showing changes across WGBS and ATAC-seq platforms (Fig. 3), several are notable. Aryl hydrocarbon receptor (*Ahr*) was hyper-methylated and located in more accessible chromatin regions in IVF ICMs. This receptor has been shown to regulate xenobiotic-metabolising enzymes such as cytochrome P450, but it is also recognised as a balancing factor for cell differentiation and function, which is controlled by levels of endogenous ligands of different affinity. For example, inflammatory mediators, glutathione depletion, reactive oxygen species and shear stress are known to function as *Ahr* activators, although with very low binding potential (Esser and Rannug, 2015). Its activation heralds the activation of a battery of xenobiotic-metabolising enzymes, many of which with inflammatory function like *Il2*, *Il1 $\beta$*  and importantly, *Il6st*. *Etv1* was hypo-methylated and located in more accessible chromatin regions in IVF ICMs. *Etv1* is a member of the E-twenty-six (ETS) transcription factor family. It is overexpressed in multiple tumours and plays an essential role in the cardiac conduction pathways (Shekhar *et al.*, 2016).

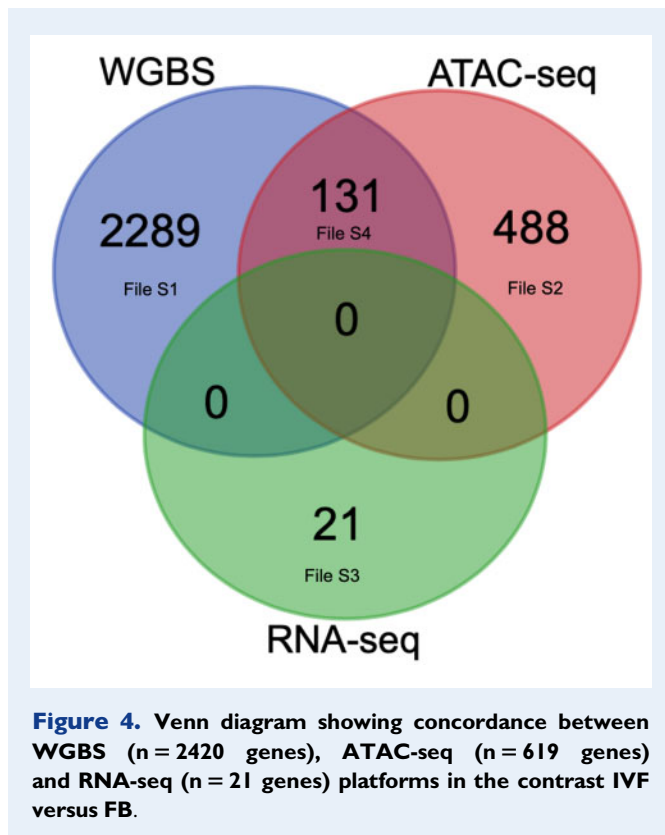
A third, important finding is related to the analysis of DNA methylation data. We found that only a very small percentage of differentially methylated CpGs induced by IVF were located in functionally

important areas like promoters (0.70%), enhancers (0.47%) or CpG islands (0.17%).

Overall, DNA methylation changes were distributed distally from the transcription start site, with the majority being located 50–500 kb from the transcription start site (TSS) (Supplementary Fig. S2B). Two-thirds were located in the gene body, specifically introns (28.67%), while the remaining third were located in intergenic regions (Fig. 2A). These findings highlight the importance of assessing DNA methylation analysis with global techniques like WGBS, as opposed to techniques that focus on querying DNA methylation changes in CpG rich areas, like reduced representation bisulfite sequencing (RRBS).

The significance of the multitude of DNA methylation changes in areas not currently known to be directly involved in gene regulation is unknown. It is possible that the observed changes might be random and have no relevant gene-regulating functions. However, it is also possible that these changes might have no significance in the early embryo, but acquire functional significance at later stages of development, particularly in specific tissues and cell types. Indeed, it has been proposed that the mammalian genome might be more accurately viewed as islands of protein-coding information in a sea of *cis*- and *trans*-acting regulatory sequences (Mattick *et al.*, 2010) and while the meaning of these changes might be escaping us, it might become evident in the future.

Although we found widespread low-level changes in DNA methylation in ICM of IVF embryos, we did not find DNA methylation differences at transposable elements (SINE, LTR and LINE, data not



shown) or in levels of DNA methylation in mtDNA. The findings of no DNA methylation changes at transposable elements are important since these elements are broadly and strongly transcribed in the early embryos and their insertions can supply new promoter, enhancer and insulator elements to protein-coding genes and establish a novel, species-specific gene regulatory networks (Gerdes et al., 2016; Ge, 2017). Similarly, although the existence of mtDNA methylation is controversial (Liu et al., 2016), the lack of DNA methylation changes in mtDNA of IVF embryos suggests epigenetic dysregulation at this locus is likely not important. Similarly, we found only a few changes in imprinted genes. Although seven imprinted genes showed differential methylation following IVF (*Adam23*, *Begain*, *Plagl1*, *Slc22a3*, *Dio3*, *Klf14* and *Sfrmbt2*), only *Plagl1* showed changes in the ICR. *Plagl1* is a known regulator of apoptosis, but functions also as a transcription factor (Varrault et al., 1998) and cofactor of regulatory proteins with epigenetic and metabolic function like HDAC1, PPAR $\gamma$ , PACAP1-R and PCAF (Vega-Benedetti et al., 2017). Of note, changes in *Plagl1* levels result in diseases. For example, *Plagl1* overexpression in human is associated with transient neonatal diabetes mellitus (Temple et al., 1996) while loss of expression is associated with severe embryonic growth restriction (Varrault et al., 2006) and development of tumours later in life (Abdollahi et al., 1997).

Of note, a subgroup of differentially methylated genes in our data set was found to be differentially methylated in other datasets, underscoring the importance of these genes. For example, the epigenetic clock (Horvath, 2013), a set of 353 CpG sites that together describe tissue age, shared 34 (10%) differentially methylated genes with our IVF versus FB. In addition, 73% (1767/2420) of our differentially methylated genes corresponded to genes identified by Colaneri et al. (2013) as being important in developmental programming.

The fourth important finding is that we found minimal differences in epigenetic signature and no gene expression changes in male versus female embryos. This is important, given the significant sexual dimorphic effect found after culturing embryos *in vitro* (Feuer et al., 2014a). Sex is, in fact, one of the cardinal characteristics determining predisposition to disease (Ober et al., 2008). During the preimplantation period, before sex hormones can have an effect, a sex bias exists in the expression level of both sex chromosome-encoded genes and autosomal genes. For example, prior global gene expression studies at the blastocyst stage have found that only 11 genes in mice (Kobayashi et al., 2006) and 53 genes in cattle (Bermejo-Alvarez et al., 2010) were differentially expressed more than 2-fold in male versus female embryos.

WGBS data indicated that 2.6% of DMR differ between male compared to female embryos; overall male embryos showed increased methylation (89%). Similarly, to the comparison of IVF versus FB, the methylation changes were located in the gene body (68.04%) in particular introns (26.80%); the remaining were intergenic, distal to CpG islands (Fig. 2B). Interestingly, the regulation of metabolic process was highlighted as showing sexual dimorphism (Supplementary File S5D). It is also notable that we found only a few differences among imprinted genes. Only 10 imprinted genes had any DNA methylation changes at any loci, while only *Peg3* showed differential methylation in the ICR. The significance of *Peg3* DNA methylation is unclear: although mutations in *Peg3* result in growth retardation and impairment of maternal behaviour (Li et al., 1999), no changes in *Peg3* DNA methylation were found in a cohort of ART children (Whitelaw et al., 2014).

A relevant finding is the very limited differences in accessible chromatin areas and gene expression found between male and female embryos. Only 12 genes had different chromatin accessibility in male compared to female *in-vivo* embryo, and there were 15 such genes in male compared to female *in-vitro* generated embryos. Surprisingly, only one gene *Rps3a3*, coding for Ribosomal Protein S3A, and two CPs were differentially expressed in male versus female embryos. While the significance of this specific change is unclear, it is notable that changes in transcription of ribosomal RNA were postulated to be at the basis of altered growth in mice subjected to dietary restriction *in utero* (Denisenko et al., 2016). Of note, only *Eif2s3y* was found to be differentially expressed in male and female mouse blastocysts by other investigators (Kobayashi et al., 2006). The low concordance with the other authors can likely be explained because of the different species or because we analysed only ICM gene expression as opposed to the whole blastocyst. The fact that the pathway Oct4 in mammalian embryonic stem cell pluripotency was altered, could indicate that the overall development of IVF embryos is compromised compared to controls or that developmental timing and staging of embryos was different between the groups. We favour the first explanation, since we strictly controlled for staging and timing of the embryos by using only expanded blastocysts of similar morphology. Finally, it is important to note that intragroup variation among replicates was similar among the groups, with the only exception being that the FB female ATAC-seq samples had a higher CV (~14%) compared to IVF females ATAC-seq samples (CV ~5%). While we cannot provide a molecular explanation of the lower variation in IVF female ATAC samples, the large number of replicate used (FB female n = 18; IVF female n = 12) makes it unlikely to be secondary to low sample size.

One note is needed regarding the experimental design. We cultured embryos in KSOM medium with amino acids under 5%

oxygen, 5% CO<sub>2</sub> and 90% nitrogen concentrations because this medium is felt to be optimal for mouse culture and abundant data exist on its effect on embryo development and gene and imprinted gene expression (Doherty *et al.*, 2000; Feuer *et al.*, 2017). Furthermore, KSOM is the basis for Global medium, which is widely used in human IVF.

Important advantages of this work include the analysis of the ICM of embryos as opposed to whole blastocyst, the analysis of sex as opposed to pooling of male and female embryos, and the use of three states of the art technology (WGBS, ATAC-seq and RNA-seq). Among the limitations, we were able to perform only two replicates of WGBS, given the very expensive nature of the technology. However, given the global nature of the analysis, the finding provides a trove of data for further testing.

In summary, this study provides the first comprehensive analysis of DNA methylation, chromatin accessibility and RNA expression changes induced by IVF in male and female ICMs.

Our studies are in agreement with past work showing that preimplantation embryo manipulation or culture can induce epigenetic changes (Doherty *et al.*, 2000; Shi and Haaf, 2002; Morgan *et al.*, 2008; El Hajj and Haaf, 2013; Canovas *et al.*, 2017; Mani *et al.*, 2020). Overall pathways involved in cardiac hypertrophy and stress were the most changed in WGBS and ATAC-seq platforms. In addition, limited evidence of sexual dimorphism was observed. Further studies should focus on understanding how these early changes may be linked to adult health.

## Supplementary data

Supplementary data are available at *Molecular Human Reproduction* online.

## Data availability

Requests for data can be sent to the corresponding author.

## Acknowledgments

The author wishes to thank Reuben Thomas for his bioinformatics support. Figure 3 was created with BioRender.com.

## Authors' roles

E.R., E.J.G., X.L., R.H., A.D. and P.R. performed experiments. P.R. was involved in conception and design. S.L.A., E.M., M.R.S. and P.R. were involved acquisition of data and analysis and interpretation of data. All authors approved the manuscript.

## Funding

This work was funded by R01 HD082039-01A1 to P.R. E.J.G. was supported by the Lalor Foundation Postdoctoral Fellowship and the Eunice Kennedy Shriver National Institute of Child Health & Human

Development of the NIH (Award Number F32HD094500). S.L.A. received funding from a grant by UC MEXUS-CONACYT.

## Conflict of interest

The authors report no conflict of interest.

## References

- Abdollahi A, Roberts D, Godwin AK, Schultz DC, Sonoda G, Testa JR, Hamilton TC. Identification of a zinc-finger gene at 6q25: a chromosomal region implicated in development of many solid tumors. *Oncogene* 1997;**14**:1973–1979.
- Andrews S. 2010 FastQC: a quality control tool for high throughput sequence data. <https://www.bioinformatics.babraham.ac.uk/projects/fastqc/> Karolchik-
- Aronesty E. *ea-utils: Command-Line Tools for Processing Biological Sequencing Data*. Durham, NC: Expression Analysis, 2011.
- Ashburner M, Ball CA, Blake JA, Botstein D, Butler H, Cherry JM, Davis AP, Dolinski K, Dwight SS, Eppig JT *et al.* Gene ontology: tool for the unification of biology. The Gene Ontology Consortium. *Nat Genet* 2000;**25**:25–29.
- Babak T, DeVeale B, Tsang EK, Zhou Y, Li X, Smith KS, Kukurba KR, Zhang R, Li JB, van der Kooy D *et al.* Genetic conflict reflected in tissue-specific maps of genomic imprinting in human and mouse. *Nat Genet* 2015;**47**:544–549.
- Barker DJ, Osmond C. Infant mortality, childhood nutrition, and ischaemic heart disease in England and Wales. *Lancet* 1986;**327**:1077–1081.
- Belli M, Zhang L, Liu X, Donjacour A, Ruggeri E, Palmerini MG, Nottola SA, Macchiarelli G, Rinaudo P. Oxygen concentration alters mitochondrial structure and function in in vitro fertilized preimplantation mouse embryos. *Hum Reprod* 2019;**34**:601–611.
- Bermejo-Alvarez P, Rizos D, Lonergan P, Gutierrez-Adan A. Transcriptional sexual dimorphism during preimplantation embryo development and its consequences for developmental competence and adult health and disease. *Reproduction* 2011;**141**:563–570.
- Bermejo-Alvarez P, Rizos D, Rath D, Lonergan P, Gutierrez-Adan A. Sex determines the expression level of one third of the actively expressed genes in bovine blastocysts. *Proc Natl Acad Sci USA* 2010;**107**:3394–3399.
- Bina M. Imprinted control regions include composite DNA elements consisting of the ZFP57 binding site overlapping MLL1 morphemes. *Genomics* 2017;**109**:265–273.
- Blaise E, Lin W, Liu X, Simbulan R, Kolahi KS, Petraglia F, Maltepe E, Donjacour A, Rinaudo P. Impaired placental nutrient transport in mice generated by in vitro fertilization. *Endocrinology* 2012;**153**:3457–3467.
- Boerjan ML, den Daas JH, Dieleman SJ. Embryonic origins of health: long-term effects of IVF in human and livestock. *Theriogenology* 2000;**53**:537–547.
- Bosch B, Sutcliffe A. Congenital anomalies following assisted reproductive technology. *Compl Outcomes Assist Reprod* 2017;**15**:15–23.
- Boulet SL, Kirby RS, Reefhuis J, Zhang Y, Sunderam S, Cohen B, Bernson D, Copeland G, Bailey MA, Jamieson DJ, for the States Monitoring Assisted Reproductive Technology (SMART)

- Collaborative et al. Assisted reproductive technology and birth defects among liveborn infants in Florida, Massachusetts, and Michigan, 2000-2010. *JAMA Pediatr* 2016;**170**:e154934.
- Buenrostro JD, Wu B, Chang HY, Greenleaf WJ. ATAC-seq: a method for assaying chromatin accessibility genome-wide. *Curr Protoc Mol Biol* 2015;**109**:21.29.1–21.29.9.
- Canovas S, Ross PJ, Kelsey G, Coy P. DNA methylation in embryo development: epigenetic impact of ART (assisted reproductive technologies). *Bioessays* 2017;**39**:1700106.
- Cavalcante RG, Sartor MA. annotatr: genomic regions in context. *Bioinformatics* 2017;**33**:2381–2383.
- Colaneri A, Wang T, Pagadala V, Kittur J, Staffa NG Jr, Peddada SD, Isganaitis E, Patti ME, Birnbaumer L. A minimal set of tissue-specific hypomethylated CpGs constitute epigenetic signatures of developmental programming. *PLoS One* 2013;**8**:e72670.
- Delle Piane L, Lin W, Liu X, Donjacour A, Minasi P, Revelli A, Maltepe E, Rinaudo PF. Effect of the method of conception and embryo transfer procedure on mid-gestation placenta and fetal development in an IVF mouse model. *Hum Reprod* 2010;**25**:2039–2046.
- Denisenko O, Lucas ES, Sun C, Watkins AJ, Mar D, Bomszyk K, Fleming TP. Regulation of ribosomal RNA expression across the lifespan is fine-tuned by maternal diet before implantation. *Biochim Biophys Acta* 2016;**1859**:906–913.
- Denomme MM, McCallie BR, Parks JC, Booher K, Schoolcraft WB, Katz-Jaffe MG. Inheritance of epigenetic dysregulation from male factor infertility has a direct impact on reproductive potential. *Fertil Steril* 2018;**110**:419–428.e1.
- Dobin A, Davis CA, Schlesinger F, Drenkow J, Zaleski C, Jha S, Batut P, Chaisson M, Gingeras TR. STAR: ultrafast universal RNA-seq aligner. *Bioinformatics* 2013;**29**:15–21.
- Doherty AS, Mann MR, Tremblay KD, Bartolomei MS, Schultz RM. Differential effects of culture on imprinted H19 expression in the preimplantation mouse embryo. *Biol Reprod* 2000;**62**:1526–1535.
- Donjacour A, Liu X, Lin W, Simbulan R, Rinaudo PF. In vitro fertilization affects growth and glucose metabolism in a sex-specific manner in an outbred mouse model. *Biol Reprod* 2014;**90**:80.
- Ecker DJ, Stein P, Xu Z, Williams CJ, Kopf GS, Bilker WB, Abel T, Schultz RM. Long-term effects of culture of preimplantation mouse embryos on behavior. *Proc Natl Acad Sci USA* 2004;**101**:1595–1600.
- El Hajj N, Haaf T. Epigenetic disturbances in in vitro cultured gametes and embryos: implications for human assisted reproduction. *Fertil Steril* 2013;**99**:632–641.
- Esser C, Rannug A. The aryl hydrocarbon receptor in barrier organ physiology, immunology, and toxicology. *Pharmacol Rev* 2015;**67**:259–279.
- Fernandez-Gonzalez R, Moreira P, Bilbao A, Jimenez A, Perez-Crespo M, Ramirez MA, Rodriguez De Fonseca F, Pintado B, Gutierrez-Adan A. Long-term effect of in vitro culture of mouse embryos with serum on mRNA expression of imprinting genes, development, and behavior. *Proc Natl Acad Sci USA* 2004;**101**:5880–5885.
- Feuer S, Liu X, Donjacour A, Simbulan R, Maltepe E, Rinaudo P. Common and specific transcriptional signatures in mouse embryos and adult tissues induced by in vitro procedures. *Reproduction* 2017;**153**:107–122.
- Feuer SK, Donjacour A, Simbulan RK, Lin W, Liu X, Maltepe E, Rinaudo PF. Sexually dimorphic effect of in vitro fertilization (IVF) on adult mouse fat and liver metabolomes. *Endocrinology* 2014a;**155**:4554–4567.
- Feuer SK, Liu X, Donjacour A, Lin W, Simbulan RK, Giritharan G, Piane LD, Kolahi K, Ameri K, Maltepe E et al. Use of a mouse in vitro fertilization model to understand the developmental origins of health and disease hypothesis. *Endocrinology* 2014b;**155**:1956–1969.
- Ge SX. Exploratory bioinformatics investigation reveals importance of “junk” DNA in early embryo development. *BMC Genomics* 2017;**18**:200.
- Gerdes P, Richardson SR, Mager DL, Faulkner GJ. Transposable elements in the mammalian embryo: pioneers surviving through stealth and service. *Genome Biol* 2016;**17**:100.
- Giritharan G, Talbi S, Donjacour A, Di Sebastiano F, Dobson AT, Rinaudo PF. Effect of in vitro fertilization on gene expression and development of mouse preimplantation embryos. *Reproduction* 2007;**134**:63–72.
- Gu H, Smith ZD, Bock C, Boyle P, Gnirke A, Meissner A. Preparation of reduced representation bisulfite sequencing libraries for genome-scale DNA methylation profiling. *Nat Protoc* 2011;**6**:468–481.
- Guo H, Zhu P, Yan L, Li R, Hu B, Lian Y, Yan J, Ren X, Lin S, Li J et al. The DNA methylation landscape of human early embryos. *Nature* 2014;**511**:606–610.
- Guo X-Y, Liu X-M, Jin L, Wang T-T, Ullah K, Sheng J-Z, Huang H-F. Cardiovascular and metabolic profiles of offspring conceived by assisted reproductive technologies: a systematic review and meta-analysis. *Fertil Steril* 2017;**107**:622–631.e5.
- Hansen KD, Langmead B, Irizarry RA. BSsmooth: from whole genome bisulfite sequencing reads to differentially methylated regions. *Genome Biol* 2012;**13**:R83.
- Heijmans BT, Tobi EW, Stein AD, Putter H, Blauw GJ, Susser ES, Slagboom PE, Lumey LH. Persistent epigenetic differences associated with prenatal exposure to famine in humans. *Proc Natl Acad Sci USA* 2008;**105**:17046–17049.
- Hon GC, Rajagopal N, Shen Y, McCleary DF, Yue F, Dang MD, Ren B. Epigenetic memory at embryonic enhancers identified in DNA methylation maps from adult mouse tissues. *Nat Genet* 2013;**45**:1198–1206.
- Horvath S. DNA methylation age of human tissues and cell types. *Genome Biol* 2013;**14**:R115.
- Hrdlickova R, Toloue M, Tian B. RNA-Seq methods for transcriptome analysis. *Wiley Interdiscip Rev RNA* 2017;**8**:e1364.
- Jackson RA, Gibson KA, Wu YW, Croughan MS. Perinatal outcomes in singletons following in vitro fertilization: a meta-analysis. *Obstet Gynecol* 2004;**103**:551–563.
- Jirtle RL. The Agouti mouse: a biosensor for environmental epigenomics studies investigating the developmental origins of health and disease. *Epigenomics* 2014;**6**:447–450.
- Karolchik D, Hinrichs AS, Furey TS, Roskin KM, Sugnet CW, Haussler D, Kent WJ. The UCSC Table Browser data retrieval tool. *Nucleic Acids Res* 2004;**32**:D493–D496.
- Karolchik D, Hinrichs AS, Kent WJ. *The UCSC Genome Browser*. Chapter 1 Unit 1.4. *Curr Protoc Bioinformatics*, 2012.

- Kobayashi S, Isotani A, Mise N, Yamamoto M, Fujihara Y, Kaseda K, Nakanishi T, Ikawa M, Hamada H, Abe K et al. Comparison of gene expression in male and female mouse blastocysts revealed imprinting of the X-linked gene, *Rhox5/Pem*, at preimplantation stages. *Curr Biol* 2006;**16**:166–172.
- Krueger F, Andrews SR. Bismark: a flexible aligner and methylation caller for Bisulfite-Seq applications. *Bioinformatics* 2011;**27**:1571–1572.
- Langmead B, Salzberg SL. Fast gapped-read alignment with Bowtie 2. *Nat Methods* 2012;**9**:357–359.
- Li L, Keverne EB, Aparicio SA, Ishino F, Barton SC, Surani MA. Regulation of maternal behavior and offspring growth by paternally expressed *Peg3*. *Science* 1999;**284**:330–333.
- Liao Y, Smyth GK, Shi W. The Subread aligner: fast, accurate and scalable read mapping by seed-and-vote. *Nucleic Acids Res* 2013;**41**:e108.
- Liao Y, Smyth GK, Shi W. featureCounts: an efficient general purpose program for assigning sequence reads to genomic features. *Bioinformatics* 2014;**30**:923–930.
- Liu B, Du Q, Chen L, Fu G, Li S, Fu L, Zhang X, Ma C, Bin C. CpG methylation patterns of human mitochondrial DNA. *Sci Rep* 2016;**6**:23421.
- Luke B. Pregnancy and birth outcomes in couples with infertility with and without assisted reproductive technology: with an emphasis on US population-based studies. *Am J Obstet Gynecol* 2017;**217**:270–281.
- Mani S, Ghosh J, Coutifaris C, Sapienza C, Mainigi M. Epigenetic changes and assisted reproductive technologies. *Epigenetics* 2020;**15**:12–25.
- Mattick JS, Taft RJ, Faulkner GJ. A global view of genomic information—moving beyond the gene and the master regulator. *Trends Genet* 2010;**26**:21–28.
- Matys V, Kel-Margoulis OV, Fricke E, Liebich I, Land S, Barre-Dirrie A, Reuter I, Chekmenev D, Krull M, Hornischer K et al. TRANSFAC and its module TRANSCOMP: transcriptional gene regulation in eukaryotes. *Nucleic Acids Res* 2006;**34**:D108–D110.
- McCarthy DJ, Chen Y, Smyth GK. Differential expression analysis of multifactor RNA-Seq experiments with respect to biological variation. *Nucleic Acids Res* 2012;**40**:4288–4297.
- McLean CY, Bristor D, Hiller M, Clarke SL, Schaar BT, Lowe CB, Wenger AM, Bejerano G. GREAT improves functional interpretation of cis-regulatory regions. *Nat Biotechnol* 2010;**28**:495–501.
- Meissner A, Gnirke A, Bell GW, Ramsahoye B, Lander ES, Jaenisch R. Reduced representation bisulfite sequencing for comparative high-resolution DNA methylation analysis. *Nucleic Acids Res* 2005;**33**:5868–5877.
- Meister TA, Rimoldi SF, Soria R, von Arx R, Messler FH, Sartori C, Scherrer U, Rexhaj E. Association of assisted reproductive technologies with arterial hypertension during adolescence. *J Am Coll Cardiol* 2018;**72**:1267–1274.
- Melamed N, Choufani S, Wilkins-Haug LE, Koren G, Weksberg R. Comparison of genome-wide and gene-specific DNA methylation between ART and naturally conceived pregnancies. *Epigenetics* 2015;**10**:474–483.
- Morgan HD, Jin XL, Li A, Whitelaw E, O'Neill C. The culture of zygotes to the blastocyst stage changes the postnatal expression of an epigenetically labile allele, *agouti viable yellow*, in mice. *Biol Reprod* 2008;**79**:618–623.
- Neph S, Kuehn MS, Reynolds AP, Haugen E, Thurman RE, Johnson AK, Rynes E, Maurano MT, Vierstra J, Thomas S et al. BEDOPS: high-performance genomic feature operations. *Bioinformatics* 2012;**28**:1919–1920.
- Ober C, Loisel DA, Gilad Y. Sex-specific genetic architecture of human disease. *Nat Rev Genet* 2008;**9**:911–922.
- Prantner AM, Ord T, Medvedev S, Gerton GL. High-throughput sexing of mouse blastocysts by real-time PCR using dissociation curves. *Mol Reprod Dev* 2016;**83**:6–7.
- Raudvere U, Kolberg L, Kuzmin I, Arak T, Adler P, Peterson H, Vilo J. g:Profiler: a web server for functional enrichment analysis and conversions of gene lists (2019 update). *Nucleic Acids Res* 2019;**47**:W191–W198.
- Rexhaj E, Bloch J, Jayet PY, Rimoldi SF, Dessen P, Mathieu C, Tolsa JF, Nicod P, Scherrer U, Sartori C. Fetal programming of pulmonary vascular dysfunction in mice: role of epigenetic mechanisms. *Am J Physiol Heart Circ Physiol* 2011;**301**:H247–H252.
- Rexhaj E, Paoloni-Giacobino A, Rimoldi SF, Fuster DG, Anderegg M, Somm E, Bouillet E, Allemann Y, Sartori C, Scherrer U. Mice generated by in vitro fertilization exhibit vascular dysfunction and shortened life span. *J Clin Invest* 2013;**123**:5052–5060.
- Ritchie ME, Phipson B, Wu D, Hu Y, Law CW, Shi W, Smyth GK. limma powers differential expression analyses for RNA-sequencing and microarray studies. *Nucleic Acids Res* 2015;**43**:e47.
- Robinson MD, McCarthy DJ, Smyth GK. edgeR: a Bioconductor package for differential expression analysis of digital gene expression data. *Bioinformatics* 2010;**26**:139–140.
- Servick K. Unsettled questions trail IVF's success. *Science* 2014;**345**:744–746.
- Shekhar A, Lin X, Liu FY, Zhang J, Mo H, Bastarache L, Denny JC, Cox NJ, Delmar M, Roden DM et al. Transcription factor ETV1 is essential for rapid conduction in the heart. *J Clin Invest* 2016;**126**:4444–4459.
- Shi L, Wu J. Epigenetic regulation in mammalian preimplantation embryo development. *Reprod Biol Endocrinol* 2009;**7**:59.
- Shi W, Haaf T. Aberrant methylation patterns at the two-cell stage as an indicator of early developmental failure. *Mol Reprod Dev* 2002;**63**:329–334.
- Solter D, Knowles BB. Immunosurgery of mouse blastocyst. *Proc Natl Acad Sci USA* 1975;**72**:5099–5102.
- Supek F, Bosnjak M, Skunca N, Smuc T. REVIGO summarizes and visualizes long lists of gene ontology terms. *PLoS One* 2011;**6**:e21800.
- Szczepanska K, Stanczuk L, Maleszewski M. Isolated mouse inner cell mass is unable to reconstruct trophectoderm. *Differentiation* 2011;**82**:1–8.
- Tan K, Wang Z, Zhang Z, An L, Tian J. IVF affects embryonic development in a sex-biased manner in mice. *Reproduction* 2016;**151**:443–453.
- Temple IK, Gardner RJ, Robinson DO, Kibirige MS, Ferguson AW, Baum JD, Barber JC, James RS, Shield JP. Further evidence for an imprinted gene for neonatal diabetes localised to chromosome 6q22-q23. *Hum Mol Genet* 1996;**5**:1117–1121.

- Thornburg KL, O'Tierney PF, Louey S. Review: the placenta is a programming agent for cardiovascular disease. *Placenta* 2010;**31**:S54–S59.
- Urich MA, Nery JR, Lister R, Schmitz RJ, Ecker JR. MethylC-seq library preparation for base-resolution whole-genome bisulfite sequencing. *Nat Protoc* 2015;**10**:475–483.
- Valenzuela-Alcaraz B, Serafini A, Sepulveda-Martinez A, Casals G, Rodriguez-Lopez M, Garcia-Otero L, Cruz-Lemini M, Bijmens B, Sitges M, Balasch J et al. Postnatal persistence of fetal cardiovascular remodelling associated with assisted reproductive technologies: a cohort study. *BJOG* 2019;**126**:291–298.
- van Wagtenonk-de Leeuw AM, Aerts BJ, den Daas JH. Abnormal offspring following in vitro production of bovine preimplantation embryos: a field study. *Theriogenology* 1998;**49**:883–894.
- Varrault A, Ciani E, Apiou F, Bilanges B, Hoffmann A, Pantaloni C, Bockaert J, Spengler D, Journot L. hZAC encodes a zinc finger protein with antiproliferative properties and maps to a chromosomal region frequently lost in cancer. *Proc Natl Acad Sci USA* 1998;**95**:8835–8840.
- Varrault A, Gueydan C, Delalbre A, Bellmann A, Houssami S, Aknin C, Severac D, Chotard L, Kahli M, Le Digarcher A et al. Zac1 regulates an imprinted gene network critically involved in the control of embryonic growth. *Dev Cell* 2006;**11**:711–722.
- Vega-Benedetti AF, Saucedo C, Zavattari P, Vanni R, Zugaza JL, Parada LA. PLAGL1: an important player in diverse pathological processes. *J Appl Genetics* 2017;**58**:71–78.
- Wang L, Wang S, Li W. RSeQC: quality control of RNA-seq experiments. *Bioinformatics* 2012;**28**:2184–2185.
- White CR, Denomme MM, Tekpetey FR, Feyles V, Power SG, Mann MR. High frequency of imprinted methylation errors in human preimplantation embryos. *Sci Rep* 2015;**5**:17311.
- Whitelaw N, Bhattacharya S, Hoad G, Horgan GW, Hamilton M, Haggarty P. Epigenetic status in the offspring of spontaneous and assisted conception. *Hum Reprod* 2014;**29**:1452–1458.
- Wu J, Huang B, Chen H, Yin Q, Liu Y, Xiang Y, Zhang B, Liu B, Wang Q, Xia W et al. The landscape of accessible chromatin in mammalian preimplantation embryos. *Nature* 2016;**534**:652–657.
- Wu J, Xu J, Liu B, Yao G, Wang P, Lin Z, Huang B, Wang X, Li T, Shi S et al. Chromatin analysis in human early development reveals epigenetic transition during ZGA. *Nature* 2018;**557**:256–260.
- Xu Q, Xie W. Epigenome in early mammalian development: inheritance, reprogramming and establishment. *Trends Cell Biol* 2018;**28**:237–253.
- Zhang Y, Liu T, Meyer CA, Eeckhoute J, Johnson DS, Bernstein BE, Nussbaum C, Myers RM, Brown M, Li W et al. Model-based analysis of ChIP-Seq (MACS). *Genome Biol* 2008;**9**:R137.
- Zhou J, Liu H, Gu HT, Cui YG, Zhao NN, Chen J, Gao L, Zhang Y, Liu JY. Association of cardiac development with assisted reproductive technology in childhood: a prospective single-blind pilot study. *Cell Physiol Biochem* 2014;**34**:988–1000.